J Nanostruct 15(4): 1970-1978, Autumn 2025

RESEARCH PAPER

Preparation and Evaluation of Slow-Release Mesoporous Silica Nanoparticles-Curcumin Implant for Prevention of Intra-Abdominal Adhesion

Dhiya Altememy [1†], Moosa Javdani [2†], Mohammad Amin Kaboli [3], Hossein Amini-Khoei [4], Parisa Mehreganzadeh [4], Fatemeh Driss [5], Mehrdad Karimi [6], Pegah Khosravian [4*]

[1] *Department of Pharmaceutics, College of Pharmacy, Al-Zahraa University for Women, Karbala, Iraq*

[2] *Department of Clinical Sciences, Faculty of Veterinary Medicine, Shahrekord University, 115, Shahrekord, Iran*

[3] *Student Research Committee, Department of Tissue Engineering and Applied Cell Sciences, School of Advanced Technologies in Medicine, Shahid Beheshti University of Medical Sciences, Tehran, Iran*

[4] *Medical Plants Research Center, Basic Health Sciences Institute, Shahrekord University of Medical Sciences, Shahrekord, Iran*

[5] *Department of Epidemiology and Biostatistics, School of Health, Shahrekord University of Medical Sciences, Shahrekord, Iran*

[6] *Department of Surgery, School of Medicine, Shahrekord University of Medical Sciences, Shahrekord, Iran*

ARTICLE INFO

Article History:
Received 02 June 2025
Accepted 21 September 2025
Published 01 October 2025

Keywords:
Cur
Slow-release product
Implant
Msn

ABSTRACT

In the present study, a slow-release system of mesoporous silica nanoparticles (Msn) loaded with curcumin (cur) is intended as an implant that can have a more significant effect on preventing intra-abdominal adhesion after surgery due to its longer shelf life and extended release of the drug in the intra-abdominal area. Msn were prepared and examined for physicochemical properties. Then, these prepared nanoparticles were loaded with cur. The implant was made from loaded nanoparticles and hydroxypropyl methylcellulose (HPMC) polymer by molding method. After the implant was made, its properties, such as disintegration time, thickness and swelling, surface pH, adhesion strength, and in vitro release, were evaluated. The implants (imp) were evaluated for the effect on intra-abdominal adhesion after laparotomy in the future paper. The results showed that the fabricated nanoparticles had acceptable morphological properties. Also, the fabricated implants had pH within the limits of normal tissue and suitable adhesion, swelling, and disintegration time. The highest adhesion strength was associated with imp, and the highest swelling was associated with imp/cur.

How to cite this article
Altememy D., Javdani M., Kaboli M. et al. Preparation and Evaluation of Slow-Release Mesoporous Silica Nanoparticles-Curcumin Implant for Prevention of Intra-Abdominal Adhesion. J Nanostruct, 2025; 15(4):1970-1978. DOI: 10.22052/JNS.2025.04.043

INTRODUCTION

Peritoneal adhesions are unusual connections between tissues and organs that result from damage to the peritoneal surfaces [1]. These adhesions, which form after abdominal surgeries, are also one of the biggest unresolved problems in today's world of medicine and impose significant costs on public health [2].

* *Corresponding Author Email: khosravian.p@skums.ac.ir*

In a study of 298 corpses that underwent laparotomy at least once in their lifetime, it was found that 67% had intraperitoneal adhesions, up from 93% in those who underwent laparotomy more than once [3]. According to the available evidence, adhesive bands are formed in 67% of cases of intra-abdominal surgery and 28% of cases of intra-abdominal infections [4]. These adhesions are the adverse outcome of incomplete fibrin lysis and cellular exudate after peritoneal injury. Other complications associated with adhesions include chronic pelvic pain, ureteral obstruction, and urinary incontinence [5]. Fibrosis-like adhesions develop at the site of surgical trauma a few days after surgery on the abdomen or pelvis. These fibrinous materials will either be removed entirely from the abdominal cavity or organized by macrophages and fibroblasts to form a fixed fibrotic adhesion.

Any mechanical trauma such as rough manipulation during surgery, use of retractors, surgical forceps and bandages during surgery, heat damage, contamination and infection, tissue ischemia, and external objects that cause damage to peritoneal endothelium will cause fibrotic adhesions [6, 7]. The severity of adhesion formation depends on the surgery's type and size. Other factors involved in adhesions include the intra-abdominal external object (mesh, glove powder, sutures) and the spread of gallstones during cholecystectomy [8]. Adhesions are the most common cause of bowel obstruction in the Western world [9].

Data analysis from several studies in this regard has shown that adhesive bands cause about 1.3 cases of intestinal obstruction, and 60% of obstruction cases are small intestines [6]. Approximately 64-79% of patients with bowel obstruction have abdominal or pelvis surgery [10].

The leading cause of more than 10% of infertility in women is the formation of these adhesions [9]. Abdominal adhesions make it impossible to perform peritoneal dialysis in patients with chronic renal failure (CRF) and also make it difficult for general surgeons to perform surgery, increasing postoperative complications [11]. However, the advanced technique of laparoscopic surgery is complex due to abdominal adhesions and even impossible in some cases [12]. Intra-peritoneal adhesions can also limit the effect of intra-peritoneal therapeutic agents used to treat cancer [5].

Abdominal adhesions also increase the surgery time, blood loss, and other complications in reoperation [11]. Due to the importance of this subject, many drugs and methods have been evaluated and tested to reduce these adhesions, and 440,000 new ideas are evaluated annually by scientists to solve this problem [13]. However, a completely effective solution to this problem has yet to be found [14]. Studies have shown that compounds with anti-inflammatory, antioxidant, anticoagulant, immunomodulatory, and antifibrotic properties can effectively reduce the formation of peritoneal adhesions [14, 15].

Many studies have already shown that compounds with antioxidant properties have a significant effect on reducing intra-abdominal adhesions [16]. Cur is a natural low molecular weight polyphenol found in the turmeric rhizome, which has anti-tumour, anti-oxidant, and anti-inflammatory effects [17]. It is helpful in the wound-healing process and prevents the formation of intra-abdominal adhesions. Also, this substance, along with its many properties, has weak side effects, so the use of this compound as a drug supplement in treatment regimens for various diseases has been considered [18-20]. One of the drug delivery systems is the implant system. The primary purpose of supplying these forms is the drug's local release to increase the drug's presence and absorption in the desired location, which can be designed for slow release. Slow-release dosage forms, while reducing the frequency of drug administration and its side effects, create a certain blood level in the body during the treatment to provide more effective treatment for the patient [21]. Since these compounds must enter the target site continuously and repetitively during the repair period. Therefore, in this study, a controlled drug delivery implant system is designed to significantly prevent intra-abdominal adhesions after surgery due to its extended stay in the position and prolonged drug release in the intraperitoneal area.

MATERIALS AND METHODS

Materials

Rats were obtained from the Pasteur Institute of Iran (Tehran, Iran). Hydroxy propyl methyl cellulose (HPMC) K100 and cur were obtained from Merck (Darmstadt, Hesse, Germany). Cetyl trimethyl ammonium Bromide (CTAB, 98 %) and Tetraethyl orthosilicate (TEOS, 99 %) were purchased from Sigma Aldrich (Seelze, Germany).

Other reagents and solvents were purchased from Merck (Darmstadt, Hesse, Germany).

Mesoporous silica nanoparticle preparation

One gram of CTAB is dissolved in 480 ml of distilled water and 3.5 ml of 2 M NaOH is added to the solution, and it is stirred at 1000 rpm and heated, and after the temperature of the solution reaches 80 °C, the amount of 5 ml of TEOS is added drop by drop and kept at 80°C for 2 hours. The obtained nanoparticles are washed several times with distilled water and ethanol and then calcined in an oven at 540 °C [22, 23].

Mesoporous silica nanoparticles characterization

To assess the form and surface morphology of nanoparticles, Msn were examined using the transmission electron microscope (TEM, Zeiss EM10C, 80 KV, Germany) and scanning electron microscope (SEM, FE-SEM, Tescan/ Mira, Brno, Czech Republic). Additionally, dynamic light scattering was used to evaluate the nanoparticles' size distribution and particle size (DLS, Mastersizer 2000; Malvern Instruments, Malvern, Worcestershire, UK). X-ray diffraction (XRD, STOE & Cie GmbH, Germany) analyses was used to investigate the crystal structure of Msn. To investigate the nanoparticle's pore size and surface area, the Brunauer–Emmett–The N2 adsorption-desorption device used teller (BET) method. The chemical structure of nanoparticles was studied by infrared (IR) spectroscopy recorded on a Nicolet Magna IR-550, America North (USA-Canada-Mexico), using KBr pellets.

Cur loaded Msn (Msn@cur) preparation

500 mg of Msn powder was poured into a 10 cc ethanol solution, added 500 mg of cur, and let rotate for 24 hours, then placed it in a 40 °C oven until the solvent evaporated [24].

Implant preparation

150 mg of HPMC K100 dissolve in 2 ml of 95% ethanol and disperse the obtained Msn@cur in the previous step in 5 ml of ethanol, add it to the HPMC K100 solution and place it on the magnetic stirrer. After one hour, it becomes a homogeneous and uniform solution. Sonic the resulting solution for 15 minutes and let it stir for another 30 minutes. The obtained solution was added to a plate with a diameter of 3 cm and allowed to dry at room temperature overnight. Place an inverted funnel on the plate to evaporate the solvent in a controlled manner. Finally, the dried films were removed and checked for defects or bubbles. They were wrapped in aluminium foil and stored in a glass container at room temperature for later steps. At that stage, the imp/Msn@cur was made.

To obtain imp/cur and imp/Msn, 500 mg of cur or 500 mg of Msn were added to ethanol solvent and HPMC K100 solution, respectively. Also, only free ethanol solvent was added to HPMC K100 solution to make the imp.

Implant characterization

Examination of the appearance

The prepared implant was visually inspected to confirm if it had a uniform, smooth and bubble-free surface, so other pharmacotherapeutic analyses should be performed on them.

Disintegration time

To determine the disintegration time of prepared implants, 1×2 cm^2 pieces of the implant were placed in a petri dish containing phosphate buffer with a pH of 7.4, 50 rpm and 37 °C. The disintegration time was detected visually when the implant was completely disintegrated.

Swelling index

Calliper measured implant thickness at 5 points, and their mean was recorded. To measure the weighted swelling index of the implant, the weighted implant specimen was placed on the surface of the plate and incubated at 37 °C. The swollen implant was weighed regularly to reach its maximum and stable weight. Implant weighted swelling index was calculated with the following formula:

$$\% \text{ weighted swelling index} = [(W_f - W_0) / W_0] \times 100$$

W_f: final implant weight

W_0: first implant weight

On the other hand, the implant thickness was measured by a calliper at 5 different points, and their mean was recorded. After the swollen process, the implants were measured again, and this formula calculated the volumetric swelling index:

$$\% \text{ volumetric swelling index} = [(V_f - V_0) / V_0] \times 100$$

V_f: final implant weight

V_0: first implant weight

Surface pH

The surface pH of the implant was determined to evaluate the possibility of mucosal stimulation by the implant. Thus, the implant sample was placed in 5 ml of phosphate buffer with pH 7.4, and the pH was measured at intervals of 2, 4 and 6 hours by placing a pH meter on the surface of the swollen implant.

In vitro adhesion strength

There are several in vitro methods for measuring the adhesion strength of an implant, often based on measuring the force required to separate the implant from a smooth surface. For this purpose, to calculate the minimum adhesion force created between the implant and the mucosa, a piece of cellulose membrane cut in the dimensions of 2×1 cm^2 was first glued to the base glass surface. In this test, we used a double bottom scale.

After the membrane was hydrated with distilled water, the implant, which was attached to the scale plate, was pressed against the surface of the membrane and remained in contact with it for one minute. Water was then added dropwise to the collector, which was in another scale plate at a 3 ml/min rate. Adding water was stopped immediately after removing the implant from the membrane surface, and the adhesion strength was calculated. This experiment was repeated three times, and its mean number was recorded.

In vitro release

Pieces of 2×1 cm^2 from the prepared implant are poured into a 12,000 Dalton dialysis bag, add 5 ml of phosphate buffer with pH 7.4, and place it in a container with 50 ml phosphate buffer: ethanol (60:40) and %0.5 tween 80 with pH 7.4, 37 °C and 100 RPM. At intervals such as 0.5, 1, 2, 3, 4, 5, 6, 12, 24, 48, 72, 96 and 120 hours, 1 ml of sample was taken and 1 ml of fresh buffer was added. The collected samples were measured by UV spectrophotometer at 422 nm and repeated thrice.

Methods of data analysis

The experimental data that underwent statistical analysis were expressed as mean ± standard deviation (SD). A statistically significant difference was deemed to exist when the p-value was less than 0.05.

RESULTS AND DISCUSSION

TEM, SEM, DLS, XRD, BET and FTIR results of Msn

Msn's surface and morphological properties were examined with TEM and SEM methods. As Figs. 1A and 1B, the particle size was about 50-100 nm. The TEM image showed the porosity and channel arrangement. Moreover, the SEM image confirmed the particles' spherical shape and uniform distribution. However, equal dispersity of Msn was seen in prepared imp/Msn@cur as Fig. 1C.

DLS analysis graphs obtained from Msn showed satisfactory dispersion (PDI = 0.285). Also, the hydrodynamic diameter reported by DLS was 287 nm, the size for water-coated nanoparticles (Fig. 2A). XRD results show Msn index peaks at 2.25, 4.1, and 5.1, confirming the nanoparticles' hexagonal and honeycomb states and crystallinity (Fig. 2B).

The mesoporous structure of Msn was confirmed by obtained isotherms of BET and BJH analysis (Fig. 2C). Isotherm diagrams in mesoporous nanoparticles have four properties:

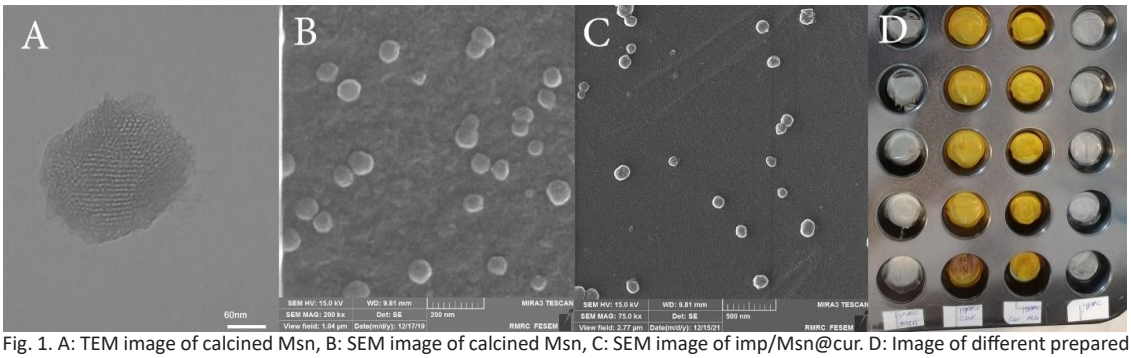

Fig. 1. A: TEM image of calcined Msn, B: SEM image of calcined Msn, C: SEM image of imp/Msn@cur. D: Image of different prepared implants.

1- Existence of distance between adsorption and desorption branch, 2- Higher desorption branch than adsorption branch, 3- Sigmoid shape and 4- high surface area. The results of BET analysis show the surface area as 778.73 m^2/g (Fig. 2D), and the effects of BJH analysis confirmed the presence of mesoporous particles with the pore radius as 1.64 nm, which is consistent with MCM-41 nanoparticles (Fig. 2E).

FTIR confirmed the chemical structure of Msn. The FTIR spectrum is shown in Fig. 3. It can be attributed to O–H stretches from 3300-2500 cm^{-1} belonging to the Msn surface OH groups. Also, the small peak at 1630.64 cm^{-1} was related to the bending frequency of OH. Also, the functional indicator groups of Msn as Si–O–Si and Si–OH showed the absorption spectra of stretching vibration at 968.99 and 810.16 cm^{-1}, respectively. Moreover, the tensile frequency of the Si-O group was seen at the peak of 810.16 cm^{-1}.

Appearance, disintegration time, swelling index, surface pH, adhesion strength and in vitro release characteristics of prepared implant

The prepared implant was examined visually. The prepared film had a uniform, smooth, bubble-free surface, opaque and yellow (Fig. 1D). However, they were ready for other pharmaceutic analyses to be performed on them.

The performance of a drug is primarily

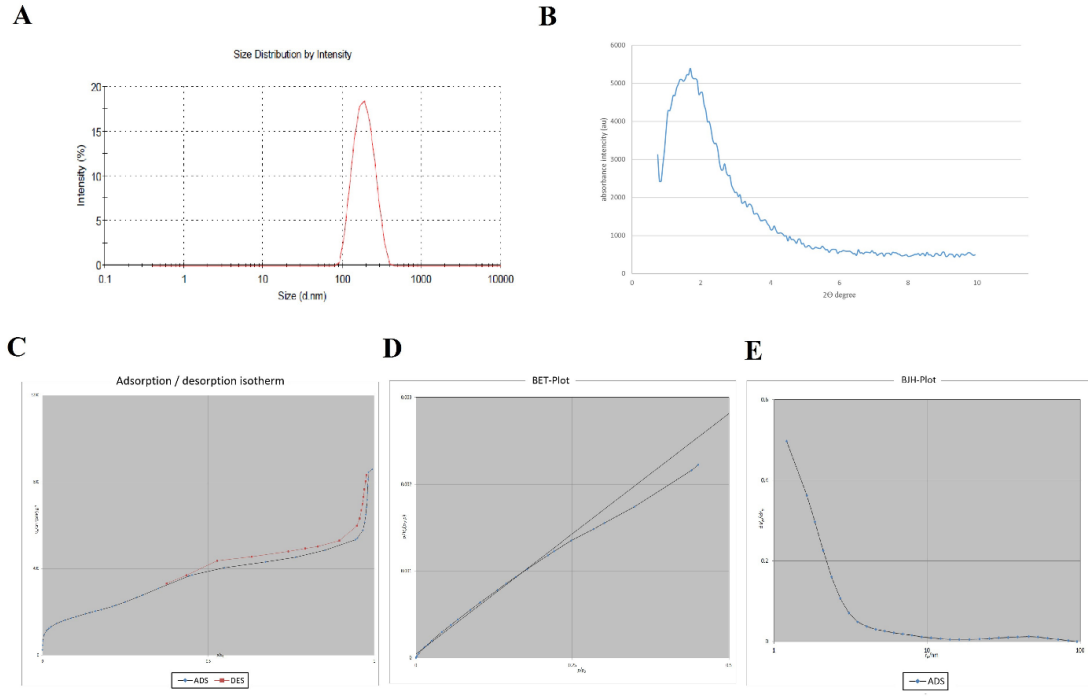

Fig. 2. A: DLS, B: XRD, C: Isotherm, D: BET and E: BJH of Msn.

Table 1. Disintegration time, weighted and volumetric swelling index, surface pH and adhesion strength of different prepared implants.

Implant type	Disintegration time (min)	weighted swelling index (%)	Volumetric swelling index (%)	2 h surface pH (mv)	4 h surface pH (mv)	6 h surface pH (mv)	adhesion strength (g)
imp/Msn@cur	60.66 ± 4.04	1529	164	7.20	7.29	7.27	162.66 ± 10.40
imp/cur	47.33 ± 1.53	2800	164	7.49	7.34	7.51	215.66 ± 17.24
imp/Msn	53 ± 3	11016	524	6.91	7.02	7.04	244.66 ± 49.66
imp	56.66 ± 1.52	3312	164	7.11	7.11	7.05	185.66 ± 46.33

influenced by the disintegration and dissolution behaviour of the dosage form. The disintegration time of the implant was determined to evaluate this dosage form disintegration in the scheduled timetable when placed in the prescribed test condition. As Table 1 shows, all types of implants were disintegrated within an hour. This result confirmed that the implants were distributed in the abdominal area, and the surfaces of all intra-abdominal organs were exposed to the cur inside the implant.

The swelling index investigation of prepared implants was done using the mentioned method. The weighty and volumetric swelling indexes were calculated using the following formula, and the obtained results are reported in Table 1.

The surface pH of the implant was determined to evaluate the possibility of mucosal stimulation by the implant. Thus, the implant sample was placed in 5 ml of phosphate buffer with pH = 7.4, and the pH was measured at intervals of 2, 4 and 6 hours by placing a pH meter on the surface of the swollen implant. The results in Table 1 show that all types of implants have a pH within the range of normal tissue, and the implant has no pH-induced side effects.

The adhesion strength of the prepared implants was performed according to the mentioned. As Table 1, the obtained results show that the prepared implant has adhesive strength and, after intraperitoneal loading, can be attached to the surrounding tissues and placed in the abdominal cavity.

Fig. 4 shows the outcomes of drug release from patches. In the first 4 hours, around 75.8% and 49.5%, respectively, of the cur was released from imp/cur and imp/Msn@cur. They both stand explosive cur release. According to the imp/Msn@cur release diagram, drug release was seen for up to 5 days, which is much less time than imp/cur. This difference may be attributable to Msn's controlled release profile instead of imp/burst cur's release from the HPMC matrix. Additionally, the percentage of cur released on day five from the two implants was roughly 91.3% and 81.3%, respectively. This shows that the patch has disintegrated, and the majority of the drug content has been released.

One of the most critical complications of intra-abdominal surgery is the formation of adhesive bands. Adhesive bands are pathological connections between the surface of the peritoneum, the viscera, and the pelvic cavity, depending on the location of the abdominal and pelvic adhesions. These adhesions form during the repair of peritoneal surface damage. However, adhesions may develop after any abdominal surgery, such as cholecystectomy, gastrectomy,

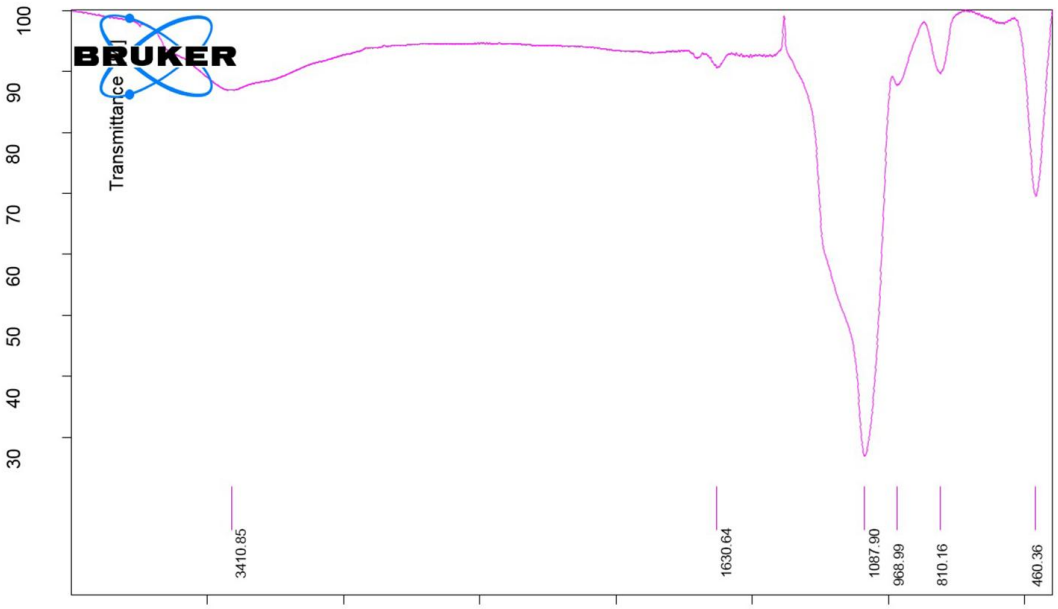

Fig. 3. FTIR spectrum of calcined Msn.

and abdominal vascular surgery [25]. One of the drug delivery systems is the implant system. The primary purpose of these dosage forms is to release the drug locally to increase the presence and absorption of the drug at the site, which can be designed to slow release [26].

Since it is necessary to deliver these compounds continuously and repetitively to the target site during the repair period, in this study, a controlled drug delivery implant system is designed to prevent intra-abdominal adhesions after surgery significantly.

Therefore, the present study was designed to implant slow-release systems of Msn loaded with cur extract as an implant that can have a more significant effect on the prevention of intra-abdominal adhesion after surgery due to having longer retention and long-term release of the drug in the intra-abdominal area.

In this study, Msn was constructed and put in an internal implant for controlled drug release of cur for prevention of intra-abdominal adhesions after surgery. Successfully synthesizing well-dispersed Msn with a particle size of around 100 nm and pore radius of about 1.64 nm demonstrated their ability to encapsulate cur in their mesopores. The synthesis of Msn as the MCM41 structure was confirmed by the spherical shape and properties of the synthesized Msn, as illustrated in Figs. 1 and 2. It was discovered that imp/Msn@cur had a lower burst release and release rate than imp/cur. Therefore, the regulated release of Msn was caused by hydrogen bond attraction between silanol groups at the pores and surfaces of Msn. As a result, the administration of MSN and the resulting imp/Msn@cur have a long-term release of cur.

Examination of the adhesive strength of the prepared implants also showed that the ready implant has adhesive strength; the highest adhesive strength is related to imp/Msn (244.6 g), imp/cur (215.6 g), imp (185.6 g), and finally imp/Msn@cur (162.6 g).

Examination of the degree of implant swelling showed that the highest swelling index is related to implants containing nanoparticles and implants

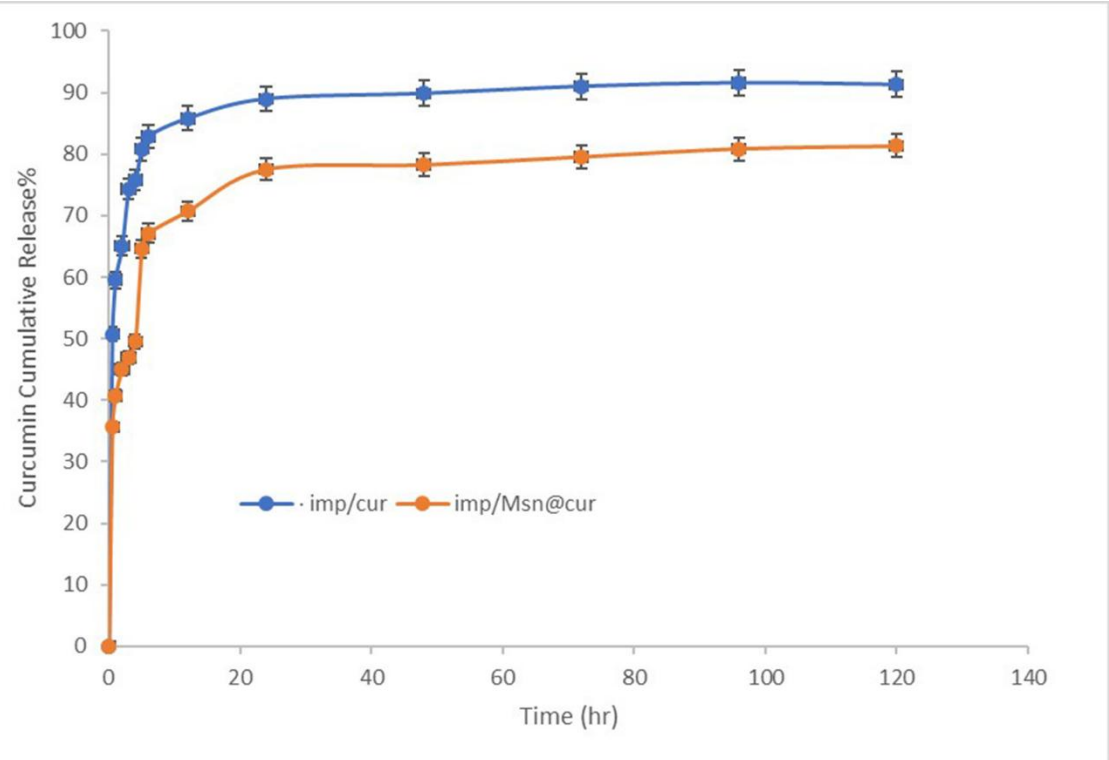

Fig. 4. In vitro cur release of imp/cur and imp/Msn@cur.

without nanoparticles, followed by implants containing cur.

Determination of the disintegration time of implant prepared in vitro showed that disintegration time was related to implant containing cur and nanoparticles, implant without nanoparticles, implant containing nanoparticles and finally, implant having cur, respectively.

The results of the present study also showed that the manufactured nanoparticles had a size between 50-100 nm. Studies have shown that nanoparticles smaller than 10 nm can be rapidly excreted through the renal excretory system or vascular leakage. In contrast, much larger nanoparticles may more likely be detected and passed by the single-nucleus phagocyte system [27]. Therefore, to maximize the effect of increasing permeability and maintenance and effective escape from physiological barriers, many studies consider the approximate size between 10 and 250 nm suitable for drug delivery purposes [28].

Mesoporous nanoparticles have very suitable dimensions for drug delivery purposes. In this study, electron microscope images confirmed the spherical shape and uniform distribution of particles. The particle size was about 100-50 nm. In this study, after loading the nanoparticles, the properties of the created nano-system were investigated.

The encapsulation efficiency of cur in mesoporous nanoparticles was about 50%, which shows a stable and excellent formulation and good maintenance during this period. Also, the loading capacity was about 50%, which indicates that the nanoparticle loading was effective and had an acceptable ratio. Also, regarding the surface pH of the implant, the results showed that the surface pH is in the range of normal tissue pH and has no destructive or irritating effect on the tissue, just as no tissue damage or stimulation was observed during the experiment in rats.

Consistent with the results of the present study, Tsai et al. Loaded 47% of cur in polylactic glycolic acid nanoparticles and produced nanoparticles with a size of 163 nm [29].

In another study by Akhtar et al., They could load cur on chitosan nanoparticles. The size of nanoparticles in their study was 218 nm, more significant than the nanoparticles made in the present study [30, 31].

Yallapu et al. Also, cur was loaded into polylactic nanoparticles of co-glycolic acid. They made 76 nanometer nanoparticles. The charge of these nanoparticles was positive 0.06 mV. They could load 69% of cur into polylactic glycolic acid nanoparticles. Their findings showed that cur efficiently loaded into smaller polylactic nanoparticles. The positive charge of nanoparticles facilitates binding these nanoparticles to negatively charged molecules at the cell surface and accelerates the transfer of cur to the target tissue [32].

Cur has many medicinal properties such as antioxidant, anti-mutant, anti-tumor anti-cancer, anti-angiogenic, anti-cholesterol and anti-bacterial properties. Still, despite its potent medicinal properties, it cannot be widely used in treating diseases. It cannot dissolve in water and, consequently, has poor bioavailability in the body environment. Various reports state that the solubility of cur increases when dissolved or encapsulated in some drug carriers [33].

CONCLUSION

There has been considerable interest in designing and developing novel intraperitoneal adhesion formulations. Using implants, mesoporous nanoparticles enhance the aqueous solubility of hydrophobic drugs and improve the drug loading capacity, therapeutic efficacy, and sustained release. Herein, we loaded the Msns with cur to prepare the slow-release implants. The results of the present study showed that the prepared implant properties, such as pH, adhesion, swelling, disintegration time, and long and controlled release of the cur. These findings suggest imp/Msn@cur as a promising intra-abdominal adhesion drug delivery candidate.

ACKNOWLEDGEMENTS

This article results from a research project as 5023 project number and IR.SKUMS.REC.1398.140 ethical code in Shahrekord University of Medical Sciences. We want to thank the Vice Chancellor for Research and Technology of Shahrekord University of Medical Sciences for financing this research, as well as the staff of the Phytochemical Laboratory at the Shahrekord University of Medical Sciences Research Center for Medicinal Plants who cooperated in implementing this project. The Iranian government funded this research by the Vice Chancellor for Research and Technology of Shahrekord University of Medical Sciences grant

number 3138. Moreover, supplement 4067 and 5305 grant numbers were used for this project.

CONFLICT OF INTEREST

The authors declare that there is no conflict of interests regarding the publication of this manuscript.

REFERENCES

1. Celepli, S., et al., The effect of oral honey and pollen on postoperative intraabdominal adhesions. The Turkish Journal of Gastroenterology, 2011. 22(1): p. 65-72.
2. Sikirica, V., et al., The inpatient burden of abdominal and gynecological adhesiolysis in the US. BMC Surgery, 2011. 11(1).
3. Weibel, M.A. and G. Majno, Peritoneal adhesions and their relation to abdominal surgery. The American Journal of Surgery, 1973. 126(3): p. 345-353.
4. Schein, M., Schwartz's Principles of Surgery, F. Charles Brunicardi, Dana K. Andersen, Timothy R. Billiar, David L. Dunn, John G. Hunter, Jeffrey B. Matthews, Raphael E. Pollock (Eds). World Journal of Surgery, 2010. 34(4): p. 871-873.
5. Monk, B.J., M.L. Berman, and F.J. Montz, Adhesions after extensive gynecologic surgery: Clinical significance, etiology, and prevention. American Journal of Obstetrics and Gynecology, 1994. 170(5): p. 1396-1403.
6. Ellis, H., The causes and prevention of intestinal adhesions. Journal of British Surgery, 1982. 69(5): p. 241-243.
7. DeCherney, A.H. and G.S. diZerega, Clinical Problem of Intraperitoneal Postsurgical Adhesion Formation Following General Urgery and The Use of Adhesion Prevention Barriers. Surgical Clinics of North America, 1997. 77(3): p. 671-688.
8. Johnston, S., et al., The need to retrieve the dropped stone during laparoscopic cholecystectomy. The American Journal of Surgery, 1994. 167(6): p. 608-610.
9. Suid-Afrikaanse Tydskrif vir Taalkunde Voorskrifte aan Skrywers. South African Journal of Linguistics, 1992. 10(3): p. 185-185.
10. Cox, M.R., et al., The Safety And Duration of Non-Operative Treatment for Adhesive Small Bowel Obstruction. Australian and New Zealand Journal of Surgery, 1993. 63(5): p. 367-371.
11. van der Krabben, A.A., et al., Morbidity and mortality of inadvertent enterotomy during adhesiotomy. Journal of British Surgery, 2000. 87(4): p. 467-471.
12. Weissenborn, K., Recent developments in the pathophysiology and treatment of hepatic encephalopathy. Baillière's Clinical Gastroenterology, 1992. 6(3): p. 609-630.
13. Liakakos, T., et al., Peritoneal Adhesions: Etiology, Pathophysiology, and Clinical Significance. Digestive Surgery, 2001. 18(4): p. 260-273.
14. Ward, B.C. and A. Panitch, Abdominal Adhesions: Current and Novel Therapies. Journal of Surgical Research, 2011. 165(1): p. 91-111.
15. Kamel, R.M., Prevention of postoperative peritoneal adhesions. European Journal of Obstetrics & Gynecology and Reproductive Biology, 2010. 150(2): p. 111-118.
16. Parsaei, P., et al., Bioactive components and preventive effect of green tea (Camellia sinensis) extract on post-laparotomy intra-abdominal adhesion in rats. International Journal of Surgery, 2013. 11(9): p. 811-815.
17. Evaluation Of Curcumin Effects On Bad, Bak, And Bim: A Molecular Dynamics Simulation Study. Journal of Pharmaceutical Negative Results, 2022. 13(3).
18. Liu, J., et al., Recent Progress in Studying Curcumin and its Nano-preparations for Cancer Therapy. Current Pharmaceutical Design, 2013. 19(11): p. 1974-1993.
19. Bansal, S.S., et al., Curcumin implants for continuous systemic delivery: safety and biocompatibility. Drug Delivery and Translational Research, 2011. 1(4): p. 332-341.
20. Khosravian, P., S. Heidari-Soureshjani, and Q. Yang, Effects of medicinal plants on radiolabeling and biodistribution of diagnostic radiopharmaceuticals: A systematic review. Plant Science Today, 2019. 6(2): p. 123-131.
21. Khosravian-Dehkordi, P., et al., In vitro antiviral activity of curcumin-loaded selenium nanoparticles against human herpes virus type 1. Journal of Shahrekord University of Medical Sciences, 2024. 26(2): p. 73-77.
22. In-vitro Evaluation of Metronidazole loaded Mesoporous Silica Nanoparticles Against Trichomonas Vaginalis. International Journal of Pharmaceutical Research, 2020. 12(sp1).
23. Najafi, A., et al., Antimicrobial action of mesoporous silica nanoparticles loaded with cefepime and meropenem separately against multidrug-resistant (MDR) Acinetobacter baumannii. Journal of Drug Delivery Science and Technology, 2021. 65: p. 102757.
24. Kaboli, M.A., et al., Silk Fibroin-Coated Mesoporous Silica Nanoparticles Enhance 6-Thioguanine Delivery and Cytotoxicity in Breast Cancer Cells. International Journal of Applied Pharmaceutics, 2025: p. 275-283.
25. Yang, Y., et al., Diosmetin exerts anti-oxidative, anti-inflammatory and anti-apoptotic effects to protect against endotoxin-induced acute hepatic failure in mice. Oncotarget, 2017. 8(19): p. 30723-30733.
26. Kaboli, M.A., et al., Investigating The Role of Nanoparticle-Based Curcumin Implants In Prevention of Post-Laparotomy Peritoneal Adhesion: An In Vivo Study. International Journal of Applied Pharmaceutics, 2024: p. 327-332.
27. Kim, W.H., et al., Effect of anticancer drugs and desferrioxamine in combination with radiation on hepatoma cell lines. Yonsei Medical Journal, 1993. 34(1): p. 45.
28. Petros, R.A. and J.M. DeSimone, Strategies in the design of nanoparticles for therapeutic applications. Nature Reviews Drug Discovery, 2010. 9(8): p. 615-627.
29. Tsai, Y.-M., et al., Curcumin and its nano-formulation: The kinetics of tissue distribution and blood–brain barrier penetration. International Journal of Pharmaceutics, 2011. 416(1): p. 331-338.
30. Akhtar, F., M.M.A. Rizvi, and S.K. Kar, Oral delivery of curcumin bound to chitosan nanoparticles cured Plasmodium yoelii infected mice. Biotechnology Advances, 2012. 30(1): p. 310-320.
31. Houshmand, F., et al., Chitosan Coated Selenium-Donepezil Nanoparticles Ameliorate Scopolamine-Induced Memory Impairment in Rats. International Journal of Applied Pharmaceutics, 2025: p. 456-467.
32. Yallapu, M.M., et al., Fabrication of curcumin encapsulated PLGA nanoparticles for improved therapeutic effects in metastatic cancer cells. Journal of Colloid and Interface Science, 2010. 351(1): p. 19-29.
33. Bharali, D.J., et al., Nanoparticle Delivery of Natural Products in the Prevention and Treatment of Cancers: Current Status and Future Prospects. Cancers, 2011. 3(4): p. 4024-4045.